
**Liquid Crystals**
Publication details, including instructions for authors and subscription information:
http://www.informaworld.com/smpp/title~content=t713926090

# Simulations of energy and switching in AFLCDs with different boundary conditions

Artur Adamski Corresponding author[a]; Herman Pauwels[a]; Kristiaan Neyts[a]
[a] LCD Research Group, ELIS Department, Ghent University, 9000 Gent, Belgium

Online publication date: 25 May 2010

**To cite this Article** Adamski Corresponding author, Artur , Pauwels, Herman and Neyts, Kristiaan(2004) 'Simulations of energy and switching in AFLCDs with different boundary conditions', Liquid Crystals, 31: 7, 997 — 1005
**To link to this Article: DOI:** 10.1080/02678290410001712532
**URL:** http://dx.doi.org/10.1080/02678290410001712532

LIQUID CRYSTALS, VOL. 31, NO. 7, JULY 2004, 997–1005



# Simulations of energy and switching in AFLCDs with different boundary conditions

ARTUR ADAMSKI*, HERMAN PAUWELS and KRISTIAAN NEYTS
LCD Research Group, ELIS Department, Ghent University,
St. Pietersnieuwstraat 41, 9000 Gent, Belgium

(*Received 12 August 2003; in final form 15 February 2004; accepted 8 March 2004*)

Using standard expressions for the various terms in the Gibbs free energy, the switching in antiferroelectric liquid crystal (AFLC) displays is simulated and the time evolution of various energy terms and of the liquid crystal director distributions are calculated. It is shown that when returning from a strong positive voltage to zero, one can reach two types of antiferroelectric state: the normal alternating state with the two bulk polarizations perpendicular to the electrodes and opposite to each other, and the alternative splayed symmetric state with two bulk polarizations parallel to the electrodes and again opposite to each other. The former case gives rise to tri-state switching characteristics, the latter to V-shaped switching. In general strong polar interaction with the alignment layer favours V-shaped switching while weak or no polar interaction give rise to tri-state switching characteristics. Since the V-shaped characteristic has so far only been demonstrated experimentally in ferroelectric liquid crystals (or antiferroelectric liquid crystals being in the ferroelectric state), the difference in AFLCs is discussed and the conditions for continuous switching are modelled. The simulations show that the switching characteristics of the antiferroelectric display can be controlled by the surface parameters.



## 1. Introduction

Since the first report of the continuous switching of smectic material there have been several years of discussion about this phenomenon, including theoretical and experimental work. In 1995 Fukuda [1] and somewhat later Inui *et al*. [2] discovered that in some three-component antiferroelectric liquid crystal (AFLC) mixtures the hysteresis loop narrowed and changed its shape for an almost linear switching characteristic similar to at exhibited by nematic materials. This experiment attracted great interest because of the possibility of using an analogue grey scale in AFLC displays. This hysteresis-free behaviour has been named 'thresholdless' and corresponds with the so-called V-shaped switching characteristic. Later other groups, for example [3], proved that this kind of switching is observed only with the synclinic state, thus it is not a feature of the antiferroelectric material. Since then there has been an intensive experimental study of the behaviour of V-shaped switching, including the investigation of bulk optical properties [4], electrostatics [5] and the influence of ions [6]. Theoretical modelling of FLC [7, 8] and AFLC thresholdless switching [9, 10] have been presented with slightly different approaches; however the simulation results reach similar conclusions. In contrast to the simulation results there is so far no experimental evidence for V-shaped switching in AFLCs. Recent experiments show, however, the importance of the cell parameters (in particular the alignment layers) in V-shaped switching characteristics [11]. Following this approach we have constructed a model in which various material and surface parameters can be scanned, and the energy evolution of the system observed, which determines the director profile and switching mode of the display.

The orientation of molecules inside the liquid crystal is governed by the energy distribution inside the layer. The molecules find themselves the most favourable energetic states, which are determined mainly by the external electric field and the boundary conditions of the display. The total molecular energy consists of the following contributions: electric energy, distortion energy, surface energy and antiferroelectric energy. It is interesting to observe the evolution and exchange of various kinds of energy during the reorientation of molecules and to compare their stationary levels. It transpires that the energy concentrated in the surface layers can determine the switching mode of the display, and the surface interactions thus play an important role in switching.

V-shaped switching in ferroelectric materials is well understood and has already been studied by several authors [7,8]. The conclusions from the simulations are

*Author for correspondence; adamsart@elis.ugent.be

*Liquid Crystals* ISSN 0267-8292 print/ISSN 1366-5855 online © 2004 Taylor & Francis Ltd
http://www.tandf.co.uk/journals
DOI: 10.1080/02678290410001712532

confirmed by experimental results and show that synclinic materials arranged in a twisted state exhibit thresholdless switching. Surfaces induce a twist of the molecular director and the polarization charge homogenizes the bulk in the sense that the spontaneous polarization vector aligns parallel to the electrodes in the field-free state. In antiferroelectric materials, however, there are two equally possible anticlinic states at zero-field: namely the normal alternating state (NA-state where the molecules are arranged so that their directors in the bulk span the plane parallel to the electrodes — horizontal arrangement), and the splayed state (SS-state where the directors span the plane perpendicular to the electrodes — vertical arrangement). Therefore the polarization vectors in the bulk are perpendicular to the electrodes and opposite to each other in the NA-state, while they are parallel to the electrodes and still opposite to each other in the SS-state. Since the horizontal case will never give continuous switching for obvious reasons, the only possibility is to determine the conditions for obtaining vertical arrangement. We have constructed a model which simulates the continuous reorientation of the director, keeping the anticlinic order by finding some special set of parameters. The energy difference between these two cases is very small, thus slight changes in the parameters may decide which of these states is reached. Both states may be locally stable but one can be 'more stable' than the other and thus may cause wall motion within a pixel [12,13]. Some parameters, however, may enhance the energy difference between the states, and thus the stability of the display. In general one can state that strong polar interaction with the alignment layer favours V-shaped switching, while weak or no polar interaction give rise to tri-state switching characteristics.

The work presented by Mottram and Elston [9] treats similar problems from a slightly different perspective. They compare the quasi-static results of the energies at zero-voltage ground state, showing five different stationary solutions. In this paper we investigate the dynamics of switching and thus the time evolution of the energy during the reorientation process. We usually start from a switched state and look for the conditions in which the system relaxes to the various anticlinic/synclinic/other states. In addition we observe the director profile during switching.

Parry-Jones and Elston introduced into their model a new quadrupolar term which stabilizes the synclinic state of the antiferroelectric material [14]. We do not include that term, because our model assumes the anticlinic state as the only stable one in the unconfined bulk. Since V-shape characteristics are usually observed close to the phase transition (SmC–SmC$_A$) one indeed should consider some local energy minimum for synclinic orientation at higher temperatures. But we assume that V-shaped switching is observed far away from the SmC to SmC$_A$ transition, and thus only in the stable anticlinic phase; in our model this quadrupolar term is therefore not taken into account. In our case the surfaces induce local stability for symmetric director reorientation and may cause a continuous transition during the relaxation process.

## 2. Energy expressions

In figure 1 the structure of an antiferroelectric liquid crystal cell is shown. It comprises the bottom and top electrodes, the two alignment layers with total thickness $d_{al}$ and the liquid crystal layer with thickness $d$. The smectic layers are assumed to have a bookshelf structure with the layers coinciding with the plane of figure 1. The orientations of the permanent polarizations $\mathbf{P}_S$ within successive layers are indicated by $\varphi_1$ and $\varphi_2$, which are the representations of the molecular angles on the smectic cone. Since the thickness of the layers is microscopic (nm) and the dimensions of the cell are macroscopic (μm) the electric field is determined by the polarization averaged over two consecutive layers and the analysis becomes one-dimensional.

Under constant voltage over the cell, the energy of the cell is the Gibbs free energy with the expression [10]:

$$\begin{aligned} G = & \int_d -E\frac{1}{2}(P_S\cos\varphi_1 + P_S\cos\varphi_2)\,\mathrm{d}x - \int_{d+d_{al}} \frac{1}{2}E\varepsilon_{xx}\varepsilon_0 E\,\mathrm{d}x \\ & + \frac{\alpha}{4}\int_d \left[\left(\frac{d\varphi_1}{\mathrm{d}x}\right)^2 + \left(\frac{d\varphi_2}{\mathrm{d}x}\right)^2\right]\mathrm{d}x \\ & - \gamma_1\frac{1}{2}(\cos^2\varphi_{1b} + \cos^2\varphi_{2b}) - \gamma_1\frac{1}{2}(\cos^2\varphi_{1t} + \cos^2\varphi_{2t}) \\ & + \gamma_2\frac{1}{2}(\cos\varphi_{1b} + \cos\varphi_{2b}) - \gamma_2\frac{1}{2}(\cos\varphi_{1t} + \cos\varphi_{2t}) \\ & + \int_d A[\cos(\varphi_1 - \varphi_2)]\,\mathrm{d}x \quad . \end{aligned} \tag{1}$$

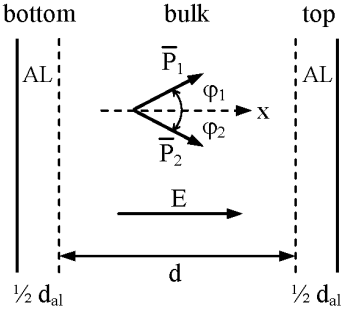


Figure 1. Antiferroelectric liquid crystal cell with bottom and top electrodes, alignment layer, liquid crystal slab and orientation of polarization in successive layers. The smectic layers have the bookshelf structure and the smectic layer plane coincides with the figure plane.

The terms on the first line will be called electric energy ($F_E$); the term $\int \frac{1}{2} E \varepsilon_{xx} \varepsilon_0 E dx$ we prefer to call electrostatic energy. The term on the second line is called distortion energy and will be denoted as $F_D$; it represents the energy of the molecules with respect to each other and is minimum for uniform alignment of the directors along the thickness. The factor ¼, instead of the usual factor ½, derives from the fact that the term with $\varphi_1$ exists only in one layer and thus in half the volume of the cell; likewise for the term with $\varphi_2$. The terms on the third and fourth line correspond to surface energy and will be denoted by $F_S$. The third line represents the non-polar interaction energy with the alignment layer. These terms are minimum for the various $\varphi$ equal to 0 or π. The terms on the fourth line represent the polar interaction energy with the alignment layer. At the bottom of the structure these terms are minimum for $\varphi_b$ equal to $\pm\pi$ (polarization $\mathbf{P}_S$ pointing into the alignment layer) and at the top of the structure they are minimum for the $\varphi_t$ equal to zero (again the polarization $\mathbf{P}_S$ pointing into the alignment layer). The factors ½ in the terms of the third and the fourth line are present because these terms exist only in one of the two consecutive layers. The final term, in the fifth line, represents the antiferroelectric interaction energy between two successive layers and will be denoted by $F_A$. This term is minimum if $\varphi_1$ and $\varphi_2$ differ by π, i.e. if the directors in two consecutive layers are at opposite sides of the smectic cone. This energy is assigned to the two layers, thus there is no factor ½. This also leads to the fact that ½$A$ of [10] plays the role of $A$ in this article, and thus $2A$ will be reflected by $4A$.

The electric field $E$ in equation (1) is not a constant over the thickness of the cell. It is the electrical induction $D$ which is a constant both over the alignment layers and the liquid crystal. Therefore, ignoring anisotropy:

$$\varepsilon\varepsilon_0 E = D - \frac{1}{2}\boldsymbol{P}_S(\cos\varphi_1 + \cos\varphi_2) \quad \text{in the liquid crystal} \tag{2a}$$

$$\varepsilon_{al}\varepsilon_0 E = D \quad \text{in the alignment layer} \tag{2b}$$

where $D$ is a constant given by:

$$V = \int_{d+d_{al}} E\,dx = \frac{D}{\varepsilon_{al}\varepsilon_0} d_{al} + \frac{D}{\varepsilon\varepsilon_0} d - \frac{\boldsymbol{P}_S}{2\varepsilon\varepsilon_0}\int_d (\cos\varphi_1 + \cos\varphi_2)\,dx \quad \text{or}$$

$$D = CV + \frac{C\boldsymbol{P}_S}{2\varepsilon\varepsilon_0}\int_d (\cos\varphi_1 + \cos\varphi_2)\,dx \quad \text{with} \quad \frac{1}{C} = \frac{d_{al}}{\varepsilon_{al}\varepsilon_0} + \frac{d}{\varepsilon\varepsilon_0}. \tag{2c}$$

## 3. Non-stationary equations

The energy expressions lead, according to Euler–Lagrange, to the following non-stationary equations [10]:

$$\eta\frac{\partial\varphi_1}{\partial t} = \alpha\frac{\partial^2\varphi_1}{\partial x^2} - E\boldsymbol{P}_S\sin\varphi_1 + 2A\sin(\varphi_1 - \varphi_2) \tag{3a}$$

$$\eta\frac{\partial\varphi_2}{\partial t} = \alpha\frac{\partial^2\varphi_2}{\partial x^2} - E\boldsymbol{P}_S\sin\varphi_2 + 2A\sin(\varphi_2 - \varphi_1) \tag{3b}$$

and to the boundary conditions:

$$\alpha\frac{\partial\varphi}{\partial x} = \gamma_1\sin 2\varphi - \gamma_2\sin\varphi \quad \text{(at bottom)} \tag{4a}$$

$$\alpha\frac{\partial\varphi}{\partial x} = -\gamma_1\sin 2\varphi - \gamma_2\sin\varphi \quad \text{(at top)} \tag{4b}$$

for both $\varphi_1$ and $\varphi_2$.

The solutions of these equations give rise to a uniform bulk state ($\varphi_u$) and two surface layers where $\varphi$ from the bulk evolves towards $\varphi$ at the interface with the alignment layers (bottom $\varphi_b$ and top $\varphi_t$). The thickness of these non-uniform surface layers [15] is of the order of the 'coherence' length $\xi = (\alpha\varepsilon\varepsilon_0)^{\frac{1}{2}}/\boldsymbol{P}_S$. A simulation program succeeds in finding these solutions, which then can be inserted into the energy expression, equation (1). One should note that in order to find a stationary stable state the total energy always evolves towards a lower energy value.

## 4. Simulation programme

In our simulation programme we start from, in principle, arbitrary initial conditions and investigate the evolution towards a new stationary state under an arbitrary constant voltage. We start from an arbitrary $\varphi$-distribution; then impose a voltage $V$ and calculate $E$ at each point along the thickness, and also $D$. These calculations are mainly based on equation (2). We then calculate the $\varphi$-distribution in the next time-step; these calculations are based on equations (3) and (4). We repeat the calculations for $E$ at each point, and for $D$, keeping $V$ constant. We continue these calculations until the stationary stable state is reached. This may

last a few hundred microseconds, but sometimes tens of milliseconds. We represent the evolution of $\varphi$ in the bulk ($\varphi_u$), the evolution of the $\varphi$-distribution along the thickness, the evolution of the energy expressions and their stationary values. For the simulations we shall consider standard values of the parameters and then consider some deviations from these values. The standard values are collected from material data sheets and from various articles which treat similar problems, for example [13]: $\mathbf{P}_S = 100\,\mathrm{nC\,cm^{-2}} = 10^{-3}\,\mathrm{C\,m^{-2}}$, $\alpha = 4\times10^{-12}\,\mathrm{J\,m^{-1}}$, $\eta = 100\,\mathrm{mPa\,s}$, $d = 1.6\times10^{-6}\,\mathrm{m}$, $d_{al} = 100\,\mathrm{nm} = 10^{-7}\,\mathrm{m}$, $A = 2000\,\mathrm{Nm^{-2}}$, $\varepsilon = \varepsilon_{al} = 5$, $\gamma_1 = \gamma_2 = 1\times10^{-4}\,\mathrm{Nm^{-1}}$, $\theta = 45^\circ$. For the transmission calculations we use a simplified formula [16]:

$$T = \sin^2\frac{\pi d\Delta n}{\lambda}\cos^2\left(\frac{\varphi_1+\varphi_2}{2}\right) \tag{5}$$

where the polarizer is oriented parallel to the smectic layer normal.

## 5. Simulation results and discussion

In previous work, the so called uniform analysis was made. In this approximation the $\varphi$-distribution is constant throughout the liquid crystal thickness and can be represented by only one variable [17]. This implies that the polar interaction energy gives no contribution and $\gamma_2 = 0$. Since strong polar interaction is needed to obtain a V-shaped switching characteristic, it is clear that the uniform theory is not a good approximation for V-shape studies. We showed however that by using a fictitious negative non-polar interaction, $\gamma_1 < 0$, one could obtain V-shape, both in ferroelectric [7] and in antiferroelectric [10] liquid crystals; this is illustrated in figure 2 (*a*). One should also take into account that in the earlier publication [17] the thickness of the alignment layer was ignored. Recent simulations of a uniform theory include an alignment layer ($d_{al} = 100\,\mathrm{nm}$) and the tri-state characteristics look quite different, figures 2 (*b*) and 2 (*c*). In fact the uniform theory then approaches the results of the non-uniform model where the symmetric state occurs within the transition from anticlinic to synclinic state.

The most important case we wish to investigate is as follows. We first apply a strong positive voltage leading to the FU-state (ferroelectric-up state in which all molecules from both layers are aligned uniformly at $\varphi = 0$, see figure 3), we then set $V = 0$ and we want to know under what conditions (1) we reach the NA-state (normal alternating state in which molecules from one layer are aligned at $\varphi = 0$ and from the other layer at $\varphi = -\pi$, see figure 3) leading to tri-state switching, and (2) when we reach the SS-state (splayed state in which bulk molecules are uniformly aligned at $\varphi = \pm\pi/2$ and the border regions are splayed within the coherence length, see figure 3) leading to V-shaped switching. We will also investigate this case by simulating stationary states under decreasing voltages. The simulations can be divided into two parts: for standard values of the parameters and large values of the parameters. The parameters varied in our simulations are the following: elastic constant coefficient $\alpha$ and two surface coefficients: polar $\gamma_2$, and non-polar $\gamma_1$ interaction.

### 5.1. *Simulations with standard parameter values*

In figures 4 to 7 we have represented the case with standard values of the parameters. Figures 4, 5 and 6 present the case with $\gamma_2 = \gamma_1$; in figure 4 the schematic transmission voltage characteristic is shown. Note the resemblance and the differences with the uniform model. In this case we reach zero-volt in the SS-state leading to a V-shaped characteristic. In figure 5 the energy evolution is shown. In figure 5 (*a*) we see the time evolution within 250 µs of the various energies during the transition from the NA- to the FU-state at $V = 12\,\mathrm{V}$. Figure 5 (*b*) shows the time evolution from FU- to the SS-state at $V = 0$; figure 5 (*c*) shows the time evolution back from the SS- to FU-state at $V = 12\,\mathrm{V}$. Note that the distortion energy and the surface energy have a different and very small scale; they have only a small influence on the total energy. Note also that the

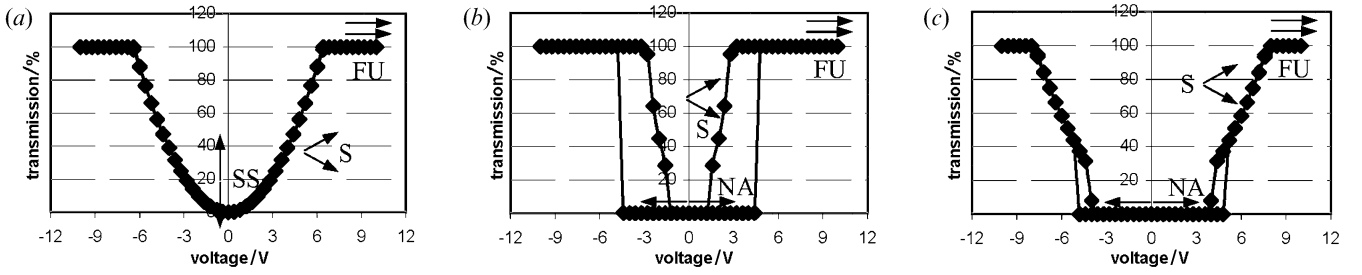


Figure 2. Simulated $T$–$V$ characteristics of a uniform model, (*a*) with negative $\gamma_1$, (*b*) without alignment layer and (*c*) with alignment layer $d_{al} = 100\,\mathrm{nm}$.

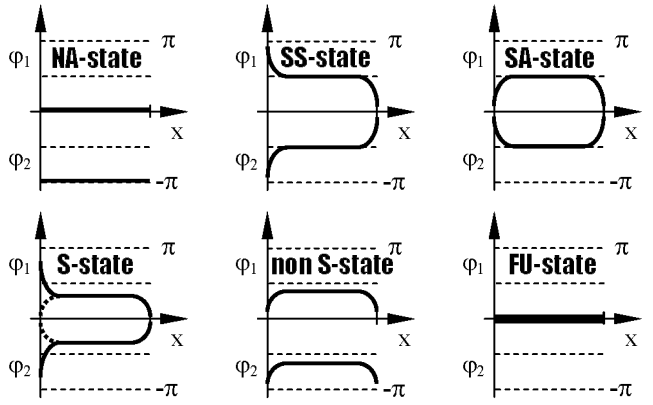


Figure 3. Possible director profiles ($\varphi$-distributions) for AFLC: normal alternating state (NA), splayed symmetric state (SS), special alternating state (SA), symmetric state (S), non-symmetric state (non-S), ferroelectric-up state (FU). The corresponding states in figures 4–11 are the representations of uniform states only.

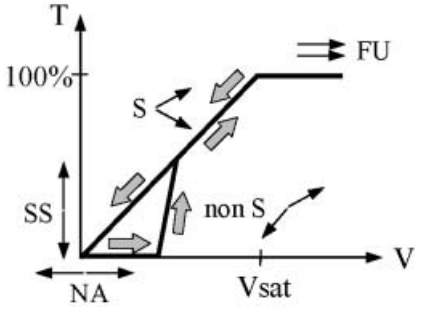


Figure 4. Schematic $T$–$V$ characteristic for the case $\gamma_1=\gamma_2=10^{-4}$ with the switching cycle: NA-state, non-S-state, S-state, FU-state; returning through the S-state ending in the SS-state, leading to V-shaped switching.

total energy always descends, which is a confirmation that the simulation programme corresponds to an energy minimization process. In figure 6 the time evolution of the $\varphi_1=-\varphi_2$ profile is shown during the transition from the FU-state to the SS-state.

The small values of the distortion and the surface energy (different scale) require some comment. For the NA-state and the SS-state, the electric energy and the antiferroelectric energy are the same for both states in the bulk; the only difference comes form the small distortion and surface energy contributions and from deviations in the surface layers (difference between bulk values and surface values of the electric and antiferroelectric energies). Therefore small variations in the model might easily change the final state.

We investigated the stability of the SS-state and the NA-state. A stable state refers to the state which does not change with time and has the same energy value for $t=0$ and $t=\infty$. The following results are based only on the simulation results, no theoretical considerations are included. Starting from the SS-state at $V=0$, we stay in this state as the time evolves. Starting from the NA-state at $V=0$ we also stay in this state. Both states are thus locally stable. However the NA-state has lower energy than the SS-state for $\gamma_2\leq 2\gamma_1$, while the SS-state has lower energy for $\gamma_2>2\gamma_1$. We tested the stability under large artificial deviations of the $\varphi$-distribution in the NA-state. The deviations in the case $\gamma_2\leq 2\gamma_1$ do not change the state, whereas for the case $\gamma_2>2\gamma_1$ the NA-stability may be broken and a slow evolution towards the SS-state can occur. The computed total energy values of all the cases mentioned above are collected in table 1(*a*). Note that the energy differences between the NA- and the SS-states are very small. If in a real experiment different domains exist in a single pixel separated by a wall, the lower energy domain will grow through wall motion. In our model, such domain walls are not included, so this phenomenon will not occur in our simulations.

In figure 7 we present the schematic $T$–$V$ characteristic for the case $\gamma_1=2.4\times10^{-4}$ and $\gamma_2=0$ giving rise to the so called SA-state (see figure 3), which is discussed in detail in [18] and will not be repeated here. It suffices to say that the SA-state requires a sufficiently large $\gamma_1$, and that the conditions for arbitrary $\gamma_1,\gamma_2$ are also mentioned in [10]. The SA-state also gives rise to the

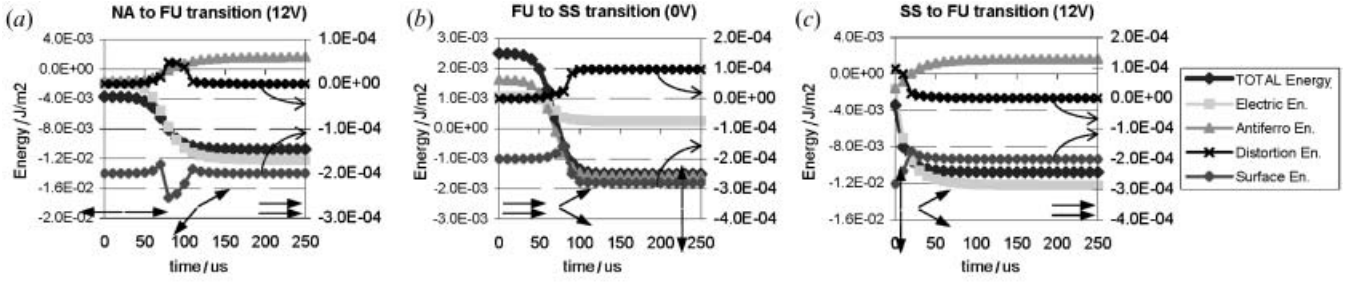


Figure 5. Energy evolution with time during V-shaped switching for standard parameter values ($\gamma\sim10^{-4}$, $\alpha\sim10^{-12}$), timescale 250 µs. Switching cycle: NA to FU (12 V), FU to SS (0 V), SS to FU (12 V), etc.

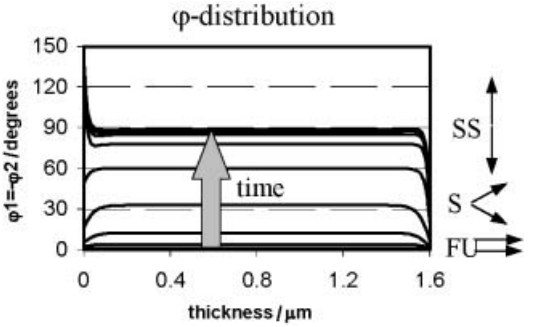


Figure 6. Time evolution of the director profile ($\varphi_1 = -\varphi_2$) during transition between FU- and SS-state for standard parameter values. Final state is a splayed state (SS) with uniform $\varphi$-distribution in the bulk ($\varphi_u = \pm\pi/2$), timescale 250 μs.

continuous switching mode but shifts the V-shaped characteristic away from its normal position. The complete simulation of all the voltages and different polarities results in the so-called W-shaped characteristic.

### 5.2. *Simulations with large parameter values*

In figures 8 to 11 we illustrate a case with larger differences between the NA- and SS-states. The small differences are caused by the small energies in the surface regions which are strongly related to the small values of the elastic constant $\alpha$ and interaction coefficients $\gamma$. We have therefore studied the case with larger values of these particular parameters, namely: $\alpha = 4 \times 10^{-10}\,\mathrm{J\,m^{-1}}$ and $\gamma_1 = 10^{-3}\,\mathrm{N\,m^{-1}}$. In this case the energy difference between the NA- and SS-states is much larger because the surface energy densities are more important and the surface regions are broader. The 'coherence' length $\xi = (\alpha\varepsilon\varepsilon_0)^{\frac{1}{2}} / \boldsymbol{P}_S$ is a measure of the width of the surface regions. We have increased the values of $\gamma$ for two reasons: (1) to increase the contribution of the surface energy to the total energy term (as mentioned above) and to let the surfaces control the switching process; (2) we took into account the condition, equation (6), to have an antiferroelectric hysteresis loop in the uniform theory, which strictly limits the values of $A$ and $\gamma$ [17],

$$A - \frac{\gamma}{d} \leq \left[\frac{\gamma}{d}\left(\frac{\gamma}{d} + A\right)\right]^{\frac{1}{2}}. \tag{6}$$

For the standard range of the $A$ parameter, the $\gamma$ value must be in the order of $\sim 10^{-3}$. In accordance with equation (4) we have also increased the value of $\alpha$ to keep $\partial\varphi/\partial x$ at the same level. With the standard values of parameters equation (6) is not fulfilled, and the holding voltage is far removed from the saturation voltage. This situation does not allow for tri-state switching, in either uniform or non-uniform approachs.

In figure 8 we have studied the case $\gamma_1 = 10^{-3}$, $\gamma_2 = 1.8 \times 10^{-3}$ and $\alpha = 4 \times 10^{-10}$. In figure 8 (*a*) we see the time evolution within 250 μs of the various energies during the transition from the NA- to the FU-state at $V = 12\,\mathrm{V}$. Figure 8 (*b*) shows the time evolution from the FU- to SS-state at $\mathrm{V} = 0$; figure 8 (*c*) shows the time evolution back from the SS- to FU-state at $V = 12\,\mathrm{V}$. Note that the energy scales are now the same for all the energies. Because the total energy is lower in this case we could state that these parameter values lead to more stable V-shaped switching. Figure 9 shows the time evolution of the $\varphi_1 = -\varphi_2$ profile during the transition from the FU-state to the SS-state. Compare the differences in the coherence length with the case of standard parameter values (figure 6).

In figure 10 we studied the case with no polar interface interaction, $\gamma_2 = 0$. Now we arrive at the NA-state giving rise to tri-state switching. At about 300 μs the transition from the FU-state to the NA-state takes place and the main driving force is the surface energy. Note that in the previous case ($\gamma$ in the range $10^{-4}$) the surface energy played a negligible role among the energy contributions and thus the final state was completely different.

The stability of the display appears quite different in this case because the parameter $\gamma_2$ clearly determines the final state, see table 1 (*b*). Starting from the NA-state, we stay in it for $\gamma_2 \leq 2\gamma_1$ and move away from it for other cases. Starting from the SS-state, we stay in it for $\gamma_2 > \gamma_1$ and move away from it for other cases. Thus the NA-state is the only one stable state for all $\gamma_2 \leq \gamma_1$ and *only tri-state* switching is possible here. Both states

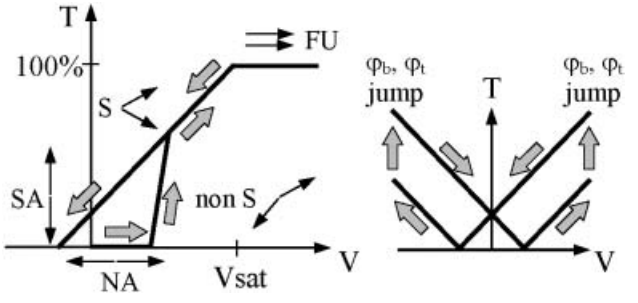


Figure 7. Schematic *TV*-characteristic for the case $\gamma_1 = 2.4 \times 10^{-4}$, $\gamma_2 = 0$ with the switching cycle: NA-state, the n-S-state, S-state, FU-state; and returning through the S-state ending in the SA-state, leading to V-shaped switching. At $\varphi_u = \pm\pi/2$ the surface values of $\varphi_b$ and $\varphi_t$ have not yet jumped to the other side. This introduces a small shift resulting in a W-form characteristic (right hand figure).

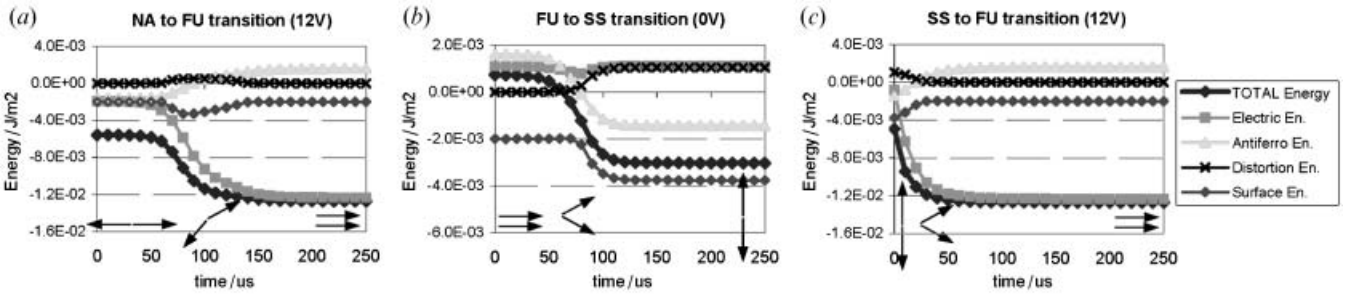


Figure 8. Energy evolution with time during V-shaped switching for large parameter values ($\gamma \sim 10^{-3}$, $\alpha \sim 10^{-10}$), timescale 250 µs. Switching cycle: NA to FU (12 V), FU to SS (0 V), SS to FU (12 V), etc.

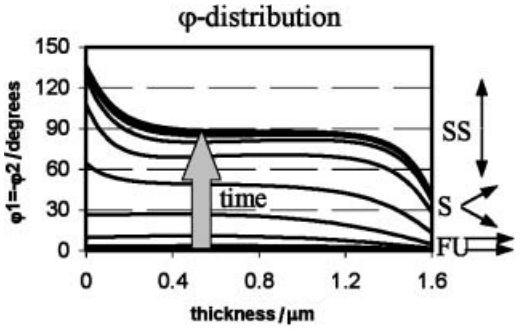


Figure 9. Time evolution of the director profile ($\varphi_1 = -\varphi_2$) during transition between FU- and SS-state for large parameter values, timescale 250 µs.

are locally stable for the case $\gamma_1 < \gamma_2 \leq 2\gamma_1$ and *both switching modes* might occur. For $\gamma_2 > 2\gamma_1$ only the SS-state becomes stable and *only the V-shape* mode is possible. Thus the stability of the display is clearly specified and the switching mode is determined by only one parameter: $\gamma_2$. Calculated values of the total energy of all the cases mentioned above are collected in table 1 (*b*). Note the energy differences between the SS- and NA-states (numbers given for $t = 0$ and $t = \infty$). Now they are very different, thus the stability of the display is improved significantly.

In figure 11 the total $T$–$V$ characteristic with a tri-state switching mode is shown and table 2 gives selected computed values of $\varphi_b$, $\varphi_u$ and $\varphi_t$ for both $\varphi_1$ and $\varphi_2$.

### 5.3. *Comparison*

We now briefly summarize the results. For standard values of $\gamma_1$ and values of $\gamma_2 > \gamma_1$, going from the FU-state we arrive at the SS-state. Again for standard values of $\gamma_1$ and for $\gamma_2 = 0$ we arrive at the so-called SA-state [18] (special alternating state, not discussed in this article, see figure 3). However for large values of parameters, $\alpha = 4 \times 10^{-10}\,\mathrm{J\,m^{-1}}$ and $\gamma_1 = 10^{-3}\,\mathrm{N\,m^{-1}}$, we reach the NA state for $\gamma_2 = 0$, and the SS-state for $\gamma_2 > \gamma_1$. The stability of the display appears quite different in the cases of standard and large parameter values (table 1). In the first case both states at 0 V are locally stable with small differences in energies, while for the second case the energies are very different and the final states are clearly separated. These results are represented in various simulation experiments.

Table 3 summarizes all the simulated cases: starting from the relaxed NA-state for standard parameter values, the liquid crystal switches between two stable states (ferroelectric-up and ferroelectric-down states) when an alternating triangle wave is applied to the cell. When the voltage reduces to 0 V the liquid crystal

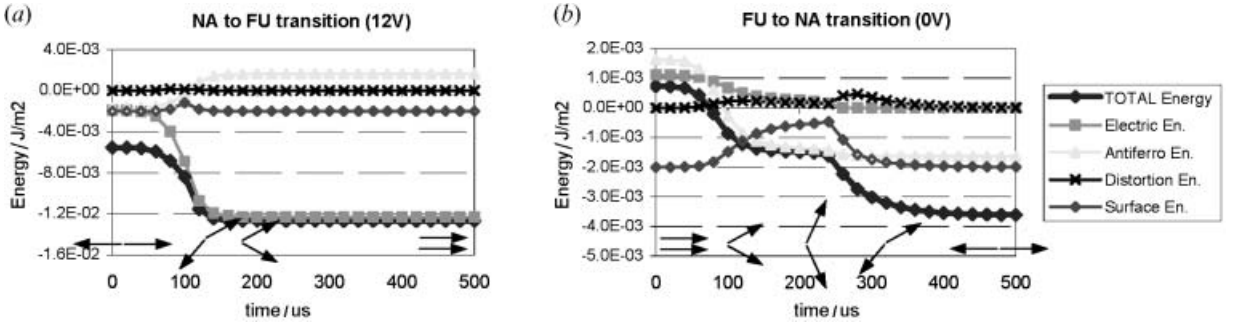


Figure 10. Energy evolution with time during tri-state switching for large parameter values and no polar interaction ($\gamma \sim 10^{-3}$, $\alpha \sim 10^{-10}$), timescale 500 µs. Switching cycle: NA to FU (12 V), FU to NA (0 V), etc.

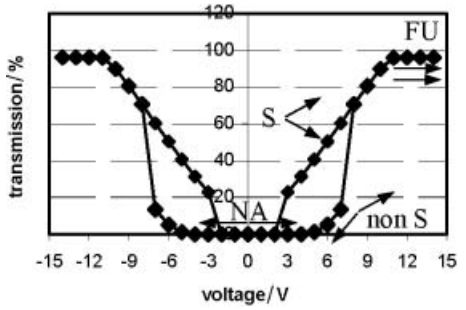


Figure 11. Simulated $T$–$V$ characteristic with tri-state switching mode for large parameter values and no polar interaction. The switching cycle: NA-state, non-S-state, S-state, FU-state; and returning through the S-state ending in the NA-state.

reaches the SS-state (or SA-state) giving rise to the continuous switching mode. This situation is the same for both strong (V-shaped) and weak (W-shaped) polar interactions. However for large parameter values the switching mode depends on the surface parameters, namely: weak polar interaction easily breaks the S-state and favours the NA-state at 0 V, giving rise to the tri-state switching characteristic, whereas strong polar interaction keeps the S-state stability much longer, reaching the SS-state at 0 V and giving rise to V-shaped switching.

## 6. Conclusions

This paper contributes to the discussion on the appearance of V-shaped characteristics in ferroelectric or antiferroelectric liquid crystals. It depends on how one returns from the FU-state with high positive voltage to the state at $V=0$. In an antiferroelectric liquid crystal one can either return to the SS-state, with both polarizations parallel to the electrodes but opposite to each other, or to the NA-state with both polarizations perpendicular to the electrodes and again opposite to each other. In a ferroelectric liquid crystal there is only one polarization and it is possible to return to a splayed state that strongly resembles the symmetric splayed state in an AFLC, except that it has only one polarization and is thus not symmetric. No alternative to the NA-state exists in ferroelectric liquid crystals; therefore if the polar interaction is strong enough there is no alternative to V-shape in a FLC.

In antiferroelectric liquid crystals, for standard values of the parameters the energy differences between the SS-state and the NA-state is small, and therefore small differences between the reality and the model may decide which of the final states one reaches: the named alternating state giving rise to a tri-state switching characteristic, or the symmetric splayed state giving rise to a V-shaped characteristic. Within the limitations of the model one can state that for strong polar interaction with the alignment layer one reaches the SS-state and thus obtains a V-shaped characteristic. If, however, the elastic constant $\alpha$ and the interface interaction coefficients $\gamma_1$ and $\gamma_2$ are larger, the energy difference between the NA-state and the SS-state becomes larger and the predictions of the model are more trustworthy: strong polar interaction gives rise to V-shaped, whereas small or no polar interaction favours tri-state switching.

The approach in this paper is purely theoretical. We simulated the hypothetical case of V-shaped switching of antiferroelectric material, keeping the anticlinic bulk order at the tip of the V (field-free state). We find that such a situation is theoretically possible, but do not know if assumed boundary conditions are realistic. At this moment very little is understood about polar and non-polar surface anchoring strengths in contact with chiral smectic material, therefore it is not easy to judge if the simulated parameters can be obtained with the present technology. Recent experiments show, however, the influence of the alignment layers on the switching characteristics, promoting V-shaped switching by strong polar surface anchoring, which is in general the same conclusion.

Table 1. Stability of the display. Energy values (in $J\,m^{-2}$) are computed for different states at $V=0$ for (*a*) standard and (*b*) large simulation parameters. Results of the stable states are given for an infinite time ($t=\infty$), results of the non-stable states are given for $t=0$.

| State | $\gamma_2=\gamma_1$ | $\gamma_2=2\gamma_1$ | $\gamma_2=5\gamma_1$ | $\gamma_2=10\gamma_1$ |
|---|---|---|---|---|
| (a) Standard simulation parameters ($\gamma\sim10^{-4}$, $\alpha\sim10^{-12}$) | | | | |
| NA | −0.00182 | −0.00182 | −0.00182 | −0.00182 |
| SS | −0.0015 | −0.00162 | −0.00211 | −0.00306 |
| (b) Large simulation parameters ($\gamma\sim10^{-3}$, $\alpha\sim10^{-10}$) | | | | |
| NA | −0.003632 | −0.003632 | unstable, evolves to SS (−0.00363) | unstable, evolves to SS (−0.00363) |
| SS | unstable, evolves to NA (−0.001839) | −0.003297 | −0.008224 | −0.017598 |

Table 2. Exact values of the calculated $\varphi$-distribution ($\varphi_u$, $\varphi_b$, $\varphi_t$) and resulting transmission ($T$) during tri-state switching. Stable states are reached starting from either (*a*) NA or (*b*) FU state and applying different voltages.

| $V$/V | $T$ % | $\varphi_{1b}$ deg | $\varphi_{1u}$ deg | $\varphi_{1t}$ deg | $\varphi_{2b}$ deg | $\varphi_{2u}$ deg | $\varphi_{2t}$ deg | Final state |
|---|---|---|---|---|---|---|---|---|
| *(a) Start from NA-state* | | | | | | | | |
| 0 | 0.0 | 0.0 | 0.0 | 0.0 | −180.0 | −180.0 | −180.0 | NA |
| 4 | 0.0 | 0.1 | 0.5 | 0.1 | −179.7 | −179.0 | −179.7 | NA |
| 5 | 1.2 | 4.0 | 13.4 | 4.0 | −170.2 | −150.6 | −170.2 | non-S |
| 7 | 13.5 | 11.5 | 36.6 | 11.5 | −135.8 | −97.7 | −135.8 | non-S |
| 8 | 70.6 | 15.9 | 35.9 | 15.9 | −15.9 | −35.9 | −15.9 | S |
| 11 | 96.0 | 0.6 | 1.8 | 0.5 | −0.6 | −1.8 | −0.5 | S |
| 12 | 96.1 | 0.0 | 0.1 | 0.0 | 0.0 | −0.1 | 0.0 | FU |
| *(b) Start from FU-state* | | | | | | | | |
| 12 | 96.1 | 0.0 | 0.1 | 0.0 | 0.0 | −0.1 | 0.0 | FU |
| 11 | 96.0 | 0.4 | 1.2 | 0.4 | −0.4 | −1.2 | −0.4 | S |
| 3 | 22.8 | 42.5 | 65.4 | 42.5 | −42.5 | −65.4 | −42.5 | S |
| 2 | 0.0 | 0.1 | 0.2 | 0.1 | −179.9 | −179.7 | −179.9 | NA |
| 0 | 0.0 | 0.0 | 0.1 | 0.0 | −180.0 | −179.9 | −180.0 | NA |

Table 3. Stable states reached after an application of a triangular waveform for standard (std) and large parameter values and resulting switching mode of the display.

| Parameter values | | $0V$ | $V_{sat}$ | $0V$ | $-V_{sat}$ | $0V$ | $V_{sat}$ | Mode |
|---|---|---|---|---|---|---|---|---|
| Std | $\gamma_2=2\gamma_1$ | NA | FU | SS | FD | SS | FU | V-shape |
| | $\gamma_2=0$ | NA | FU | SA | FD | SA | FU | W-shape |
| Large | $\gamma_2=2\gamma_1$ | NA | FU | SS | FD | SS | FU | V-shape |
| | $\gamma_2=0$ | NA | FU | NA | FD | NA | FU | tri-state |

Since the SS-state (vertical anticlinic state) has never yet been observed, we can speculate about the limitations of our model, namely: the numerical values may be out of range, the NA-state is realized only by wall motion, and smectic layer to layer interaction should have a strong threshold (quadrupolar term). These limitations could explain the contradiction between the simulation results and the present state of experiments in this field.

This work is supported by the IUAP 5/18 project and SAMPA project.

## References

[1] Fukuda, A., 1995, *Proc. IDRC*, **61,** 177.
[2] Inui, S., Iimura, N., Suzuki, T., Iwane, H., Miyachi, K., Takanishi, Y., and Fukuda, A., 1996, *J. mater. Chem.*, **6,** 671.
[3] Rudquist, P., Lagerwall, J., Buivydas, M., Gouda, F., Lagerwall, S., Clark, N., Maclennan, J., and *et al.*, 1999, *J. mater. Chem.*, **9,** 1257.
[4] Seomun, S., Gouda, T., Takanishi, Y., Ishikawa, K., Takezoe, H., and Fukuda, A., 1999, *Liq. Cryst.*, **26,** 151.
[5] Clark, N., Coleman, D., and MacLennan, J., 2000, *Liq. Cryst.*, **27,** 985.
[6] Copic, M., MacLennan, J., and Clark, N., 2001, *Phys. Rev. E*, **63,** 031703.
[7] Pauwels, H., and Lagerwall, S., 2001, *Liq. Cryst.*, **28,** 573.
[8] Copic, M., MacLennan, J. E., and Clark, N., 2002, *Phys. Rev. E*, **65,** 021708.
[9] Mottram, N., and Elston, S., 2000, *Phys. Rev. E*, **62,** 6787.
[10] Pauwels, H., 2002, *Liq. Cryst.*, **29,** 849.
[11] Chandani, A., Cui, Y., Seomun, S., Takanishi, Y., Ishikawa, K., Takezoe, H., and Fukuda, A., 1999, *Liq. Cryst.*, **26,** 167.
[12] Fornier, J., Pauwels, H., Zhang, H., and Becherelli, R., 1999, *Proc. IDRC*, 682.
[13] Fornier, J., 1997, PhD thesis ELIS Department, Ghent University.
[14] Parry-Jones, L., and Elston, S., 2001, *Appl. Phys. Lett*, **79,** 2097.
[15] Zhuang, Z., MacLennan, J. E., and Clark, N. A., 1989, *Proc. SPIE*, **1080,** 110.
[16] de Vos, A., and Reynaerts, C., 1989, *J. Appl. Phys.*, **65,** 2616.
[17] Pauwels, H., de Meyere, A., Fornier, J., and de Ley, E., 1994, *Proc. IDRC*, 495.
[18] Adamski, A., Pauwels, H., Neyts, K., Desimpel, C., and Vermael, S., 2001, *Proc. SPIE*, **4759,** 127.